Electronic structure, magnetism, and disorder in the Heusler compound Co_2TiSn

Hem Chandra Kandpal,[1] Vadim Ksenofontov,[1]
Marek Wojcik,[2] Ram Seshadri,[3] and Claudia Felser[1]

[1]Institut für Anorganische Chemie und Analytische Chemie
Johannes Gutenberg-Universität, Staudinger Weg 9, 55099 Mainz, Germany
kandpal@uni-mainz.de
[2]Institute of Physics, Polish Academy of Sciences
Al. Lotnikow 32/46, 02-668 Warszawa, Poland
[3]Materials Department and Materials Research Laboratory
University of California, Santa Barbara, CA 93106, USA

Abstract. Polycrystalline samples of the Heusler compound Co_2TiSn have been prepared and studied using bulk techniques (X-ray diffraction and magnetization) as well as local probes (^{119}Sn Mössbauer spectroscopy and ^{59}Co nuclear magnetic resonance spectroscopy) in order to determine how disorder affects half-metallic behavior and also, to establish the joint use of Mössbauer and NMR spectroscopies as a quantitative probe of local atom ordering in these compounds. Additionally, density functional electronic structure calculations on ordered and partially disordered Co_2TiSn compounds have been carried out at a number of different levels of theory in order to simultaneously understand how the particular choice of DFT scheme as well as disorder affect the computed magnetization. Our studies suggest that a sample which seems well-ordered by X-ray diffraction and magnetization measurements can possess up to 10% of antisite (Co/Ti) disordering. Computations similarly suggest that even 12.5% antisite Co/Ti disorder does not destroy the half-metallic character of this material. However, the use of an appropriate level of non-local DFT is crucial.

PACS numbers: 71.20.b, 75.50.Cc, 76.80.+y

1. Introduction

In recent years, the challenge of creating spintronic devices[1] has increasingly required, for spin valves and for spin injection, ferromagnetic materials with high Curie temperatures, high magnetic moments, and high spin polarization. These are invariably attributes of half-metallic ferromagnets.[2] A half-metal is a ferromagnet with a gap in one of the spin directions at the Fermi energy ϵ_F. Amongst the numerous compounds studied which have this property, the Heusler compounds are perhaps the most promising. Many recent investigations on bulk [3–8] and thin film [9–13] Heusler compounds have been carried out, and their use in devices has been investigated as well.[11, 14–19]

A number of electronic structural and magnetic studies have been carried out on one specific Heusler compound Co_2TiSn. For example, Majumdar *et al.*[20] have observed a semiconductor-metal transition at the Curie temperature of this compound at 350 K, for which they invoked low carrier concentration at the ϵ_F. Pierre *et al.*[21] have systematically studied the magnetic behavior of Co_2TiSn. A number of theoretical studies on this compound have also been carried out.[22–25] Despite this considerable body of theoretical and experimental work, some of the behavior of Co_2TiSn remains ambiguous.

The goal of this contribution is two-fold. We use a combination of X-ray diffraction and magnetization measurements on a well-annealed (800 K, 14 days) polycrystalline sample of Co_2TiSn to establish that it seems, by these techniques, to be well-ordered, and a full (integral) moment ferromagnet, which we treat as a criterion for it being a half-metal. We then use the *local* probes of ^{119}Sn Mössbauer spectroscopy and ^{59}Co spin-echo nuclear magnetic resonance spectroscopy to accurately establish the degree of antisite disorder in this seemingly well-ordered compound. Finally, we establish that different levels of density functional theory provide distinctly different results regarding whether the compound is half-metallic. Using the highest level of these computations, we demonstrate that as much as 12.5% antisite Co/Ti disorder does not destroy the half-metallic character.

2. Experimental and computational methods

Co_2TiSn was prepared by arc-melting the elements under an argon atmosphere after many pump/purge steps using a 10^{-4} mbar vacuum. The arc-melting procedure was repeated three times to ensure homogeneity. The product was subsequently sealed in an evacuated silica tube and annealed at 800 K for 14 days. The room temperature X-ray diffraction pattern of Co_2TiSn was measured on a Bruker D8 instrument operated in reflection geometry with a MoK$\alpha_{1,2}$ X-ray source. To improve statistics, three datasets were collected and used in the Rietveld refinement. SQUID magnetization measurements on the annealed sample were performed on a Quantum Design MPMS 5XL magnetometer. The measured saturation magnetic moment was $2\,\mu_B$ per formula

unit at 5 K.

Mössbauer measurements on powder samples were performed in the transmission geometry using a constant-acceleration spectrometer and a He bath cryostat. ^{119}Sn Mössbauer spectrum were measured using a 10 mCi ^{119}Sn ($CaSnO_3$) source. The RECOIL 1.03 Mössbauer analysis software was used to fit the experimental spectrum.[26] ^{59}Co NMR experiments on samples of powdered Co_2TiSn were carried out at 4.2 K using a broadband phase-sensitive spin-echo spectrometer.[27] The NMR spectrum was recorded by measuring spin-echo intensities. In the final NMR spectrum, the intensities were corrected for the enhancement factor and for the usual ω^2 dependence of spectrum intensity, to obtain relative intensities that are proportional to the number of nuclei with a given NMR resonance frequency. The external magnetic field was zero, and a constant excitation RF field was used.[28]

We have used a combination of four different first principles density functional theory codes: The full-potential linear augmented plane wave code WIEN2K[29] and the full-potential linear muffin tin orbital (FPLMTO) method,[30] and for comparison, the LMTO method within the atomic sphere approximation (LMTO-ASA)[31] and the spin-polarized relativistic Korringa-Kohn-Rostroker SPRKKR[32] method as well. These latter methods approximate the potential within a crystal to be a summation of spherical potentials over the atomic sites (SPRKKR) and atomic and interstitial sites (LMTO-ASA). The experimental cell parameter was used in all the calculations.

The exchange-correlation energy functional was evaluated within the local density approximation (LDA), using the von-Barth-Hedin [33] as well as generalized gradient approximation (GGA), using the Perdew-Burke-Ernzerhof [34] parametrization. Muffin-tin radii (RMTs) were taken in the range 2.3 to 2.36 a_{Bohr} for all the atoms, and this resulted in nearly touching spheres. Self-consistent calculations employed a grid of 455 irreducible k points on a $25 \times 25 \times 25$ mesh in the irreducible wedge of the Brillouin zone. This number of irreducible k points was found to be sufficient for convergence. The energy convergence criterion was set to 10^{-5}. Charge convergence was monitored concurrently.

3. Results and discussion

3.1. Experiments

Figure 1 displays the Mo-Kα X-ray powder diffraction pattern of the annealed Co_2TiSn sample. Experimental data are displayed as points. The data were subject to refinement using the Rietveld method as implemented in the XND code.[35] The gray line is the Rietveld fit ($R_{Bragg} = 3.7\%$) to the cubic $Fm\overline{3}m$ Heusler structure with a cell parameter that refined to 6.0718(3) Å. Since the atomic number of Sn ($Z = 50$) is well distinguished from the atomic numbers of Ti ($Z = 22$) and Co ($Z = 27$), we performed a number of simulations where the Sn site was partially occupied by these lighter atoms. These simulations suggested that Sn is fully ordered in this compound. The small Z

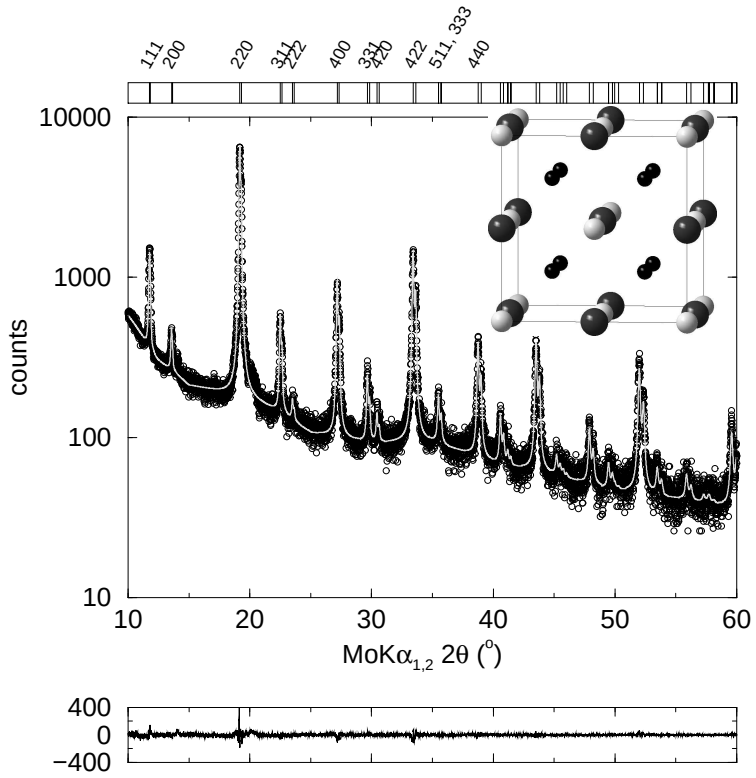

Figure 1. MoK_α X-ray powder diffraction pattern of an annealed Co_2TiSn sample, plotted on a semilog scale. Points are data, and the gray line is the Rietveld fit. The difference profile is also displayed in the panel below, in linear counts. The inset is the Heusler crystal structure showing Co atoms (small black spheres) at 8*a* ($\frac{1}{4}\frac{1}{4}\frac{1}{4}$), Ti atoms (small light-gray spheres) at 4*a* (000), and Sn atoms (large dark-gray spheres) at 4*b* ($\frac{1}{2}\frac{1}{2}\frac{1}{2}$). Vertical lines at the top of the plot are the expected α_1 and α_2 peak positions. The low angle peaks are indexed.

difference between Co and Ti did not allow for their relative occupancies in the two sites to be refined, so that in the refinement model, their occupancies were fixed to one corresponding to 8.8% antisite Co/Ti disorder as suggested by the other *local* probes presented here. The refined isotropic thermal parameters for all atoms were somewhat large but reasonable, in the range of $B = 1.4$ to $1.7\,\text{Å}^2$.

The ^{119}Sn Mössbauer spectrum of annealed sample of Co_2TiSn measured at room temperature is shown in figure 2(a). To fit the spectrum a magnetic hyperfine field distribution model was employed. The Co_2TiSn spectrum can be decomposed into three sub-spectra with the same isomer shift IS = 1.48(2) mms^{-1} and zero quadrupole splitting. The partial intensities and hyperfine magnetic fields of the three sub-spectra are provided in the caption of figure 2. A resolved hyperfine structure is revealed in the distribution $p(H)$ displayed figure 2(b). The asymmetrical distribution has a maximum at 65.9(1) kOe and small intensity at zero value of the hyperfine field. Note that the hyperfine field density distribution curve for a completely ordered compound should contain only one symmetrical peak. The asymmetry in the $p(H)$ distribution as a

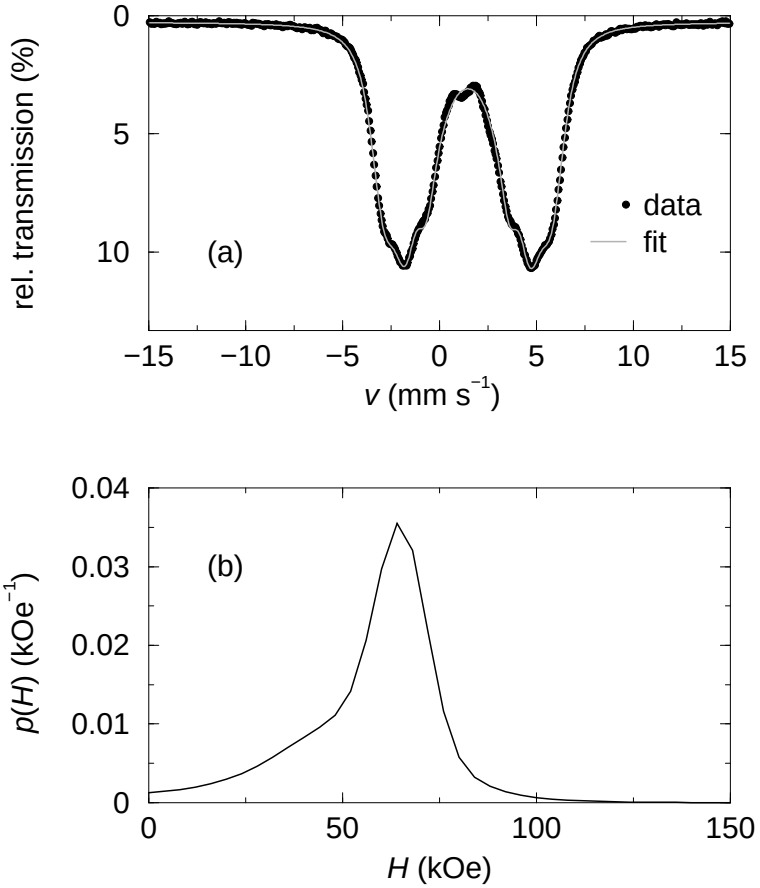

Figure 2. (a) ^{119}Sn Mössbauer spectrum of annealed Co_2TiSn sample recorded at 295 K and (b) the hyperfine magnetic field distribution on Sn atoms in Co2TiSn. The spectrum is fit using a single isomer shift but assuming the following distribution of hyperfine fields and their relative intensities: 65.9(1) kOe (49%), 56.4(8) kOe (39%), and 20(1) kOe (12%).

function of the hyperfine field suggests partial disordering of the environment around Sn. To complete the interpretation, we turn to ^{59}Co NMR spectroscopy.

The ^{59}Co NMR spectrum of Co_2TiSn acquired at 5K is presented in figure 3. The resonance frequencies f are related to the hyperfine fields (indicated on the upper abscissa) through the gyromagnetic ratio, $g = 1.0103\,\mathrm{kHz\,Oe^{-1}}$. The spectrum can be decomposed into five Gaussian peaks A through E with the parameters described in the caption. The dominant line in the spectrum at frequency $f_C = 21.1(3)$ MHz is unsplit in agreement with the cubic structure of Co_2TiSn. Two satellite lines located at $f_D = 27(3)$ MHz and $f_E = 35(4)$ MHz correspond to Co atoms experiencing higher hyperfine fields in comparison to the main line. We consider the main line as originating from Co atoms in ordered stoichiometric surroundings, whereas the satellites stem from the Co positions with Co atoms in their first coordination sphere. The first coordination sphere of Co atoms in the fully ordered structure would be 4 Ti and 4 Sn atoms. Statistical mixing of Ti and Co atoms should obey the expression for the probability to find n

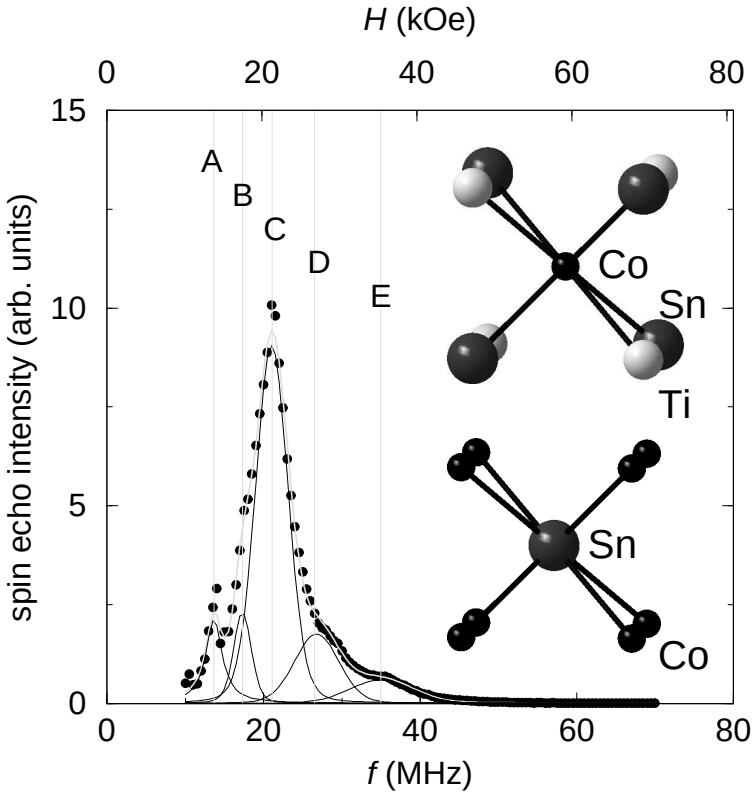

Figure 3. ^{59}Co NMR spectrum of Co_2TiSn. The data could be fit using five Gaussian peaks whose centers are indicated by vertical gray lines. The resonance frequencies (relative intensities) of the five peaks (labeled A through E) are: $f_A = 13.7(3)$ MHz (10%), $f_B = 17.3(4)$ MHz (8%), $f_C = 21.1(3)$ MHz (60%), $f_D = 27(3)$ MHz (15%), and $f_E = 35(4)$ MHz (7%). The upper abscissa displays the equivalent hyperfine fields. The insets show the (4Ti + 4Sn) coordination of Co and the 8Co coordination of Sn.

impurity atoms from amongst N neighbors using a binomial distribution:

$$W_n = \frac{N!}{n!(N-n)!}(1-x)^n x^{N-n}$$

where x is fraction of "extrinsic" atoms. For example, the probability corresponding to a single extra Co atom substituting a Ti would correspond to $N = 4$ (for the four usual Ti neighbors) and $n = 1$ (for the Co atom substituent). The distribution describing the probability of observing the "undisturbed" first coordination sphere suggests 7.8% of Co atoms substituting Ti atoms. The resonance line at $f_D = 27(3)$ MHz originates from a Co atom with one Co atom substituting one of the 4 Ti in its first coordination shell, and at $f_E = 35(4)$ MHz, the Co atoms being probed has two Co atoms substituting for Ti.

The second coordination sphere of Co atoms comprises six Co atoms. Substitution of the Co atoms in the second coordination sphere by nonmagnetic Ti atoms should decrease the hyperfine magnetic field and hence the resonance frequency. The resonance line at $f_B = 17.3(4)$ MHz is attributed to a Co having one of its six Co in the second

coordination sphere being replaced by Ti, and the line at $f_A = 13.7(3)$ MHz is then attributed to a Co with two Ti atoms, substituting for two Co atoms in its second coordination sphere. The binomial distribution model gives the amount of Ti atoms substituting Co atoms to be 8.8%. Taking into account the amount of Co atoms substituting Ti atoms, the final composition describing the antisite disordering, can be approximately written: $[Co_{(2-0.09)}Ti_{(0.09)}][Ti_{(1-0.09)}Co_{(0.09)}]Sn$ or more concisely as $(Co_{1.91}Ti_{0.09})(Ti_{0.91}Co_{0.09})Sn$.

With an understanding of disorder from NMR, we can return to the X-ray diffraction in order to understand why it is unable to discern the disorder. The exchange of Ti with Co atoms on both 8*a* positions, as suggested by NMR, is indicative of the structure being partially DO_3-like. Because both the usual Heusler ($L2_1$) and the DO_3 structure type have the same space group ($Fm\bar{3}m$), and because the atomic numbers of Ti and Co are not well separated, the determined composition $(Co_{1.91}Ti_{0.09})(Ti_{0.91}Co_{0.09})Sn$ is not easily distinguished by X-ray diffraction from pristine Co_2TiSn.

The site assignment of Sn atoms follows from the statistical analysis of intensities obtained from Mössbauer spectroscopic measurements. First coordination sphere of Sn atoms comprises eight Co atoms. Partial substitution of Co atoms by Ti atoms should diminish the hyperfine magnetic field on Sn atoms. This effect clearly follows from the hyperfine field distribution presented in the caption of figure 2. The sub-spectrum with a hyperfine field of 65.9(1) kOe can be assigned to the "undisturbed" configuration of Sn atoms. The sub-spectrum with the reduced hyperfine field of 56.4(8) kOe corresponds to Sn with seven Co and one Ti neighbors. The part of distribution with a hyperfine field of 20(1) kOe indicates the further increase in the amount of Ti atoms substituting Co atoms in the first coordination sphere of Sn; six Co and 2 Ti. The binomial distribution then suggests 8.6% of Ti atoms substituting Co on average which is in excellent agreement with the 8.8% proposed based on the ^{59}Co NMR experiment. The composition $(Co_{1.91}Ti_{0.09})(Ti_{0.91}Co_{0.09})Sn$ is therefore consistent with the ^{119}Sn Mössbauer data as well.

3.2. Computation

Densities of state of ordered Co_2TiSn obtained using the different methods are shown in figure 4. It is seen that the methods using spherical potentials (LMTO-ASA and SPRKKR) fail to obtain the correct, measured full moment, which we take here to mean a half-metallic ground state. Panel (a) of this figure shows that within these computational schemes, minority spin state are occupied. The full potential schemes embodied in the WIEN2K and FPLMTO codes however do correctly obtain a minority gap in this compound, and the full, measured magnetic moment of $2\,\mu_B$ *per* formula unit. Very little, if any, difference is seen between the two spherical potential codes, and between the two full-potential methods. The calculated moments using different codes, and using LDA and GGA are summarized in table 1. The calculated total magnetic moments are

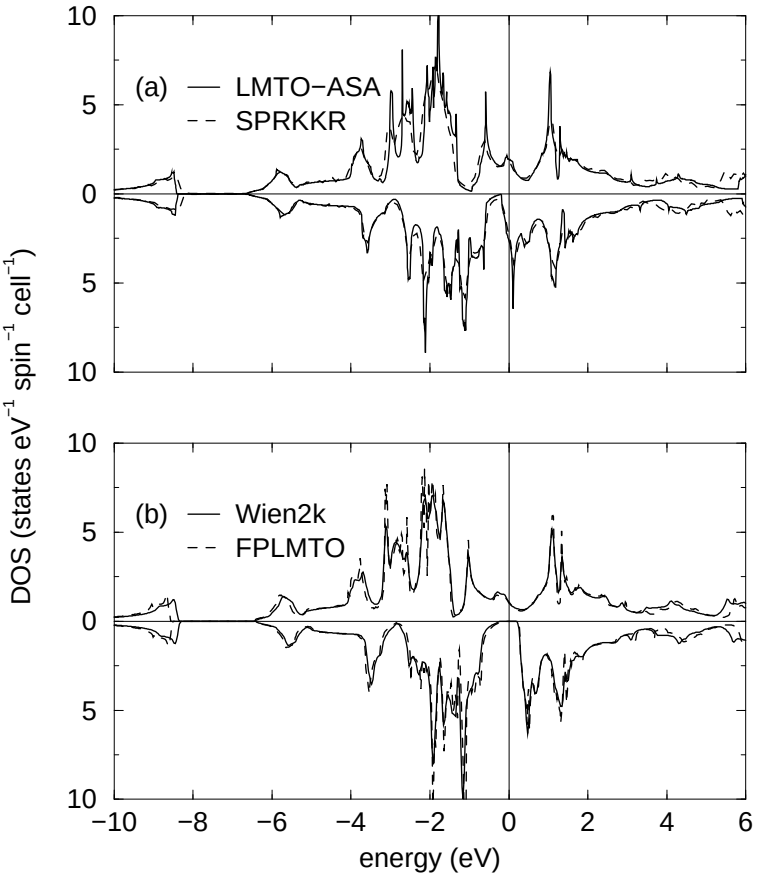

Figure 4. (a) Densities of state of ordered Co_2TiSn obtained using the LMTO-ASA and SPRKKR codes. (b) Densities of state of ordered Co_2TiSn obtained using the WIEN2K and FPLMTO codes. 0 on the energy axis is ϵ_F. All the calculations used the generalized gradient approximation.

Table 1. Magnetic moments of ordered Co_2TiSn calculated using different schemes.

Code	LDA moment (μ_B)	GGA moment (μ_B)
LMTO-ASA	0.84	1.40
SPRKKR	1.11	1.55
WIEN2K	1.99	2.00
FPLMTO	1.99	2.00

in the range from 0.84 to 2.00 μ_B. It is also noted that in addition to using full-potential methods, gradient corrections (GGA) help to obtain the correct full moment electronic structure description of this compound.

In agreement with our NMR and Mössbauer experiments, the most probable defects in Co_2TiSn are Co-Ti swap, which give rise to the general formula $(Co_{2-z}Ti_z)(Ti_{1-z}Co_z)Sn$, with z in this case being close to 0.09. Two other kinds of disorder [36] can be considered: A Co-antisite where a Ti atom is replaced by Co, and a Ti-antisite where a Co atom is replaced by Ti. We do not consider any disordering

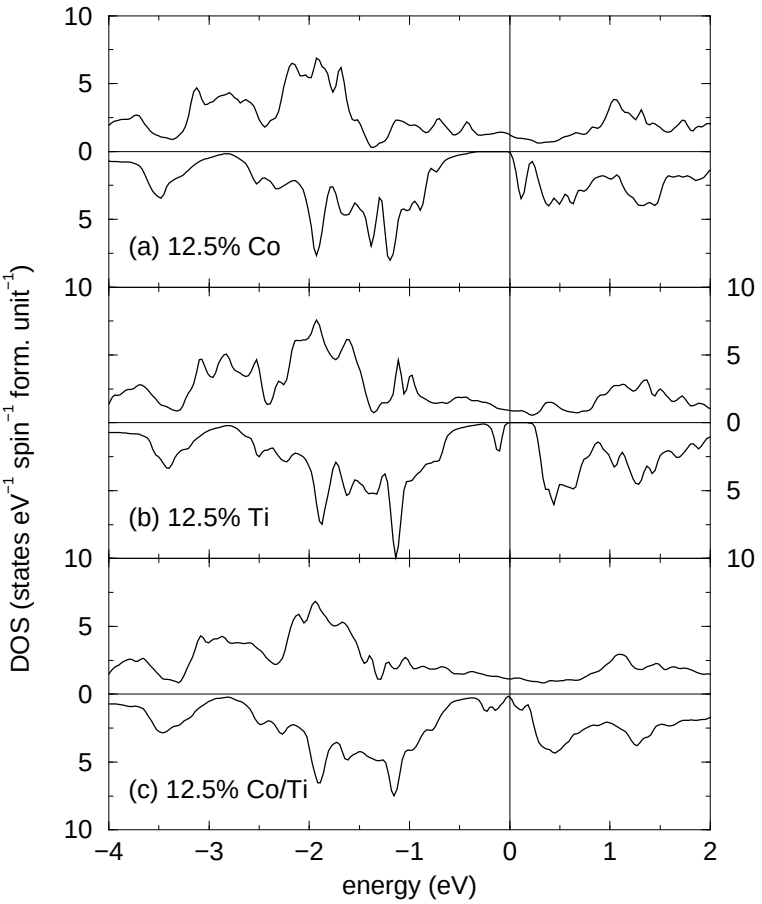

Figure 5. Densities of state of disordered Co_2TiSn obtained using the WIEN2K code: (a) 12.5% Co substituting Ti; (b) 12.5% Ti substituting Co; (c) 12.5% Co/Ti swap.

of Sn since neither the local probes, nor X-ray diffraction give any suggestion of it. We have considered all three cases of disordering in band structure calculations, with a disordering rate of 12.5%. This value was chosen because it is easily implemented in supercells involving doubling lattice parameters in all three directions. It is also close to what is experimentally observed. It should be noted that all three modes of disorder require require lowering of symmetry from cubic.

Figure 5 shows the WIEN2K-GGA densities of state, scaled to one Co_2TiSn formula unit, for the three cases of disordering. In order to focus on the gap in the minority spin direction, the data are displayed in a small window of energy around ϵ_F. It is seen that in all cases, the minority gap at ϵ_F (half-metallic character) is retained. All three modes of disorder results in new states being created in the minority gap of pure Co_2TiSn. The majority states are nearly unaffected by the disorder. Excess Co substituting for Ti is seen to create states above ϵ_F, whereas excess Ti substituting for Co is seen to create states below ϵ_F. The swapping of Co and Ti does a little of both, and the gap as a consequence, is almost lost. In general, these Heusler compounds seem to be robust half-metals. The calculations refer to zero Kelvin, and it can be expected that smearing

of states at finite temperature will further diminish the gap, and at least for the last case (c) of the Co/To swap; disorder in conjunction with finite temperatures would be deleterious for half-metallic behavior.

4. Conclusions

This work allows a number of conclusions to be drawn from the combination of experiments and computation on an important Heusler compound. From experiments, we observe that compounds that seem to be ordered, from X-ray diffraction, and from magnetization measurements, can through *local* probes such as Mössbauer and NMR be found to possess significant and quantifiable antisite disorder. In this particular case, the precise nature of the disorder is consistent with approximately 9% of Co and Ti exchanging their lattice sites. The power of Mössbauer and NMR used together in establishing local disorder has been demonstrated.

Computationally, the very interesting result is demonstrated that different implementations of density functional theory provide distinctly different results. To correctly reproduce the half-metallic ground state of Co_2TiSn, both non-local descriptions of the exchange correlation functional (GGA) as well as, more importantly, non-spherical potentials are required to be used in the calculations. Thus, it is only the full-potential methods that are able to correctly represent the electronic structure of Co_2TiSn. In agreement with experiment, the system can accommodate quite a large degree of antisite disorder without loosing its half-metallic character.

Acknowledgments

This work is financially supported by the DFG (project TP1 and TP7 in research group FG 559). RS gratefully acknowledges the National Science Foundation for support through a Career Award (DMR04-49354).

[1] Wolf S A, Awschalom D D, Buhrman R A, Daughton J M, von Molnar S, Roukes M L, Chtchelkanova A Y and Treger D M 2001 *Science* **294** 1488

[2] de Groot R A, Mueller F M, Engen P G v and Buschow K H J 1983 *Phys. Rev. Lett.* **50**(25) 2024

[3] Block T, Felser C, Jakob G, Ensling J, Mühling B, Gütlich P and Cava R J 2003 *J. Solid State Chem.* **176** 646

[4] Umetsu R Y, Kobayashi K, Kainuma R, Fujita A, Fukamichi K, Ishida K and Sakuma A 2004 *Appl. Phys. Lett.* **85** 2011

[5] Umetsu R Y, Kobayashi K, Fujita A, Oikawa K, Kainuma R, Ishida K, Endo N, Fukamichi K and Sakuma A 2005 *Phys. Rev. B* **72** 214412

[6] Wurmehl S, Fecher G H, Kandpal H C, Ksenofontov V, Felser C, Lin H-J and Morais J 2005 *Phys. Rev. B* **72** 184434

[7] Wurmehl S, Fecher G H, Kroth K, Kronast F, Dürr H A, Takeda Y, Saitoh Y, Kobayashi K, Lin H-J, Schönhense G and Felser C 2006 *J. Phys. D:Appl. Phys.* **39** 803

[8] Balke B, Fecher G H, Kandpal H C, Felser C, Kobayashi K, Ikenaga E, Kim J-J and Ueda S 2006 *Phys. Rev. B* **74** 104405

[9] Grabis J, Bergmann A, Nefedov A, Westerholt K and Zabel H 2005 *Phys. Rev. B* **72** 024437

[10] Inomata K, Okamura S, Miyazaki A, Kikuchi M, Tezuka N, Wojcik M and Jedryka E 2006 *J. Phys. D: Appl. Phys.* **39** 816
[11] Yamamoto M, Marukame T, Ishikawa T, Matsuda K, Uemura T and Arita M 2006 *J. Phys. D: Appl. Phys.* **39** 824
[12] Bergmann A, Grabis J, Nefedov A, Westerholt K and Zabel H 2006 *J. Phys. D: Appl. Phys.* **39** 842
[13] Singh L J, Barber Z H, Kohn A, Miyoshi Y, Bugoslavsky Y, Branford W R and Cohen L F 2006 *Appl. Phys. Lett.***84** 2367
[14] Kämmerer S, Thomas A, Hütten A and Reiss G 2004 *Appl. Phys. Lett.* **85** 79
[15] Okamura S, Miyazaki A, Sugimoto S, Tezuka N and Inomata K 2005 *Appl. Phys. Lett.* **86** 232503
[16] Sakuraba Y, Hattori M, Oogane M, Ando Y, Kato H, Sakuma A, Miyazaki T and Kubota H 2006 *Appl. Phys. Lett.* **88** 192508
[17] Sakuraba Y, Miyakoshi T, Oogane M, Ando Y, Sakuma A, Miyazaki T and Kubota H 2006 *Appl. Phys. Lett.* **89** 0528508
[18] Oogane M, Sakuraba Y, Nakata J, Kubota H, Ando Y, Sakuma A and Miyazaki T 2006 *J. Phys. D: Appl. Phys.* **39** 834
[19] Tezuka N, Ikeda N, Miyazaki A, Sugimoto S, Kikuchi M and Inomata K 2006 *Appl. Phys. Lett.* **89** 112514
[20] Majumdar S, Chattopadhyay M K, Sharma V K, Sokhey K J S, Roy S B and Chaddah P 2005 *Phys. Rev. B* **72** 012417
[21] Pierre J, Skolozdra R V and Stadnyk Y V 1993 *J. Magn. Magn. Mater.* **128** 93
[22] Mohn P, Blaha P and Schwarz K 1995 *J. Magn. Magn. Mater.* **140-144** 183
[23] Lee S C, Lee T D, Blaha P and Schwarz K 2005 *J. Appl. Phys.* **97** 10C307
[24] Hickey M C, Husmann A, Holmes S N and Jones G A 2006 *J. Phys.: Condens. Matter* **18** 2897
[25] Miura Y, Shirai M and Nagao K 2006 *J. Appl. Phys.* **99** 08J112
[26] Spiering H, Deak L and Bottyan L 2000 *Hyperfine Interact.* **125** 197
[27] Nadolski S, Wojcik M, Jedryka E and Nesteruk K 1995 *J. Magn. Magn. Mater.* **140-144** 2187
[28] Bibes M, Balcells L, Valencia S, Fontcuberta J, Wojcik M, Jedryka E and Nadolski S 2001 *Phys. Rev. Lett.* **87** 067210
[29] Blaha P, Schwarz K, Madsen G K H, Kvasnicka D and Luitz J 2001, WIEN2K, an augmented plane wave + local orbitals program for calculating crystal properties, `http://www.wien2k.at`
[30] Savrasov S Y and Savrasov D Y 1992 *Phys. Rev. B* **46** 12181
[31] Jepsen O and Andersen O K 2000 Stuttgart TB-LMTO-ASA program version 47 `http://www.fkf.mpg.de/andersen/`
[32] Ebert H 2005 The Munich SPR-KKR package, version 3.6, `http://olymp.cup.uni-muenchen.de/ak/ebert/sprkkr`
[33] von Barth U and Hedin L 1972 *J. Phys. C: Solid State Phys.* **5** 1629
[34] Perdew J P, Burke K and Ernzerhof M 1996 *Phys. Rev. Lett* **77** 3865
[35] Bérar J F and Baldinozzi G 1998 *IUCr CPD Newsletter* **20** 3
[36] Picozzi S, Continenza A and Freeman A J 2004 *Phys. Rev. B* **69** 094423